ACS APPLIED ENGINEERING MATERIALS

pubs.acs.org/acsaenm Article

Polymer-Derived Silicon Carbide and Boron Nitride Nanotube Composites with High Thermal Shock Resistance

Haoran Li, Leila Shahriari, Yash Khandwani, Samuel Talevich, Aspen Reyes, Rebekah Sweat, Keyou Mao, Lyndsey R. Scammell, R. Roy Whitney, Jin Gyu Park, Qiang Wu, Zhiyong Liang, and Zhibin Yu*

Cite This: *ACS Appl. Eng. Mater.* 2023, 1, 3205−3213 Read Online

ACCESS | Metrics & More | Article Recommendations | Supporting Information

ABSTRACT: Ceramic composite manufacturing typically requires high temperatures and a long duration of sintering or pyrolysis and has a low yield. Efforts to accelerate manufacturing, especially in the case of emerging polymer-derived ceramics, can result in void and crack formation or even catastrophic failure of the ceramic product. Research findings reveal that boron nitride nanotube networks effectively reinforce polymer-derived silicon carbide ceramics, enabling them to withstand substantial volume changes during pyrolysis. This reinforcement results in the production of high-quality ceramics characterized by extremely low porosity and enhanced mechanical and thermal properties, encompassing improvements in the elastic modulus, fracture strength, ductility, and thermal shock resistance. No degradation of mechanical properties was observed after 100 thermal shock cycles with a sudden temperature drop of about 1100 °C at a rate of about 2190 °C s^{-1}. By increasing the nanotube weight concentration to 40%, highly flexible ceramic thin films were obtained that can be bent to a small radius without failure. With the addition of nanotubes, pyrolysis can also proceed with a much faster temperature ramping rate for both heating and cooling cycles, enabling much faster manufacturing throughput than conventional pyrolysis for dense-structure ceramics.

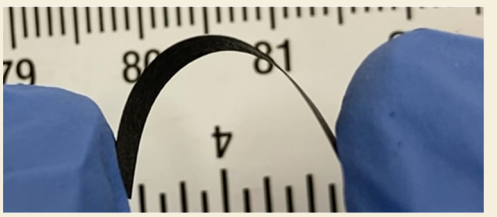

KEYWORDS: *polymer-derived ceramics, SiC, BNNTs, thermal shock, composites, extreme environments*

INTRODUCTION

Advanced materials that can withstand elevated temperature, corrosive liquids, gases, and/or energetic radiation are demanded for load-bearing and sensing applications in extreme environments, including hypersonic flights, deep space exploration, and nuclear power plants.[1,2] Ceramics and their composites have shown much better stability in such severe conditions than their polymeric and metallic counterparts. However, most ceramics are difficult to manufacture due to their much higher melting temperatures than polymers and metals. Traditional ceramic manufacturing involves solid-state sintering of ceramic powders under pressure. This process tends to create a large density of voids in the ceramics that lead to their relatively low mechanical toughness.[3] Liquid phase sintering has also been explored with lower-melting-point ceramic additives.[4] However, those additives negatively affect the high-temperature mechanical properties of the sintered ceramics.[5] In both cases, a fabricated ceramic monolith usually needs to be further machined into a specific shape and size by using additional cutting and polishing tools. This subtractive process is challenging to realize a complex three-dimensional (3D) geometry that can be desired for a customized application.

Polymer-derived ceramics (PDCs) have recently been studied as an alternative approach to manufacturing ceramic materials and composites.[6] PDCs are formed by the pyrolysis of preceramic polymers. As of now, many different polymer structures have been synthesized that have led to various types of ceramics after pyrolysis, including oxides, nitrides, carbides, their composites, etc. One unique advantage of PDCs is that the preceramic polymer part can be shaped into different forms including fibers, thin films, foams, monolithic bodies, and customized 3D objects prior to the pyrolysis process.[7,8] However, the pyrolysis of the preceramic polymer (when the polymer is converted to ceramic) results in a large volume shrinkage due to material decomposition and densification that leads to cracking or even shattering of the final ceramic sample.

To mitigate problems in PDC manufacturing, various methods can be adopted ranging from the design of the polymer composition to the polymer part's geometry to careful control of the pyrolysis conditions. For instance, preceramic polymers with high char yields can partially mitigate volume shrinkage during pyrolysis.[9,10] 3D printed cellular structures or microimprinted thin-film patterns allow the volume shrinkage to occur more uniformly and reduce the chance of cracking in a fast pyrolysis process.[11,12] However, such approaches are not applicable to compact ceramic fabrication. In most cases,

Received: September 5, 2023
Revised: November 1, 2023
Accepted: November 2, 2023
Published: November 15, 2023

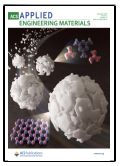

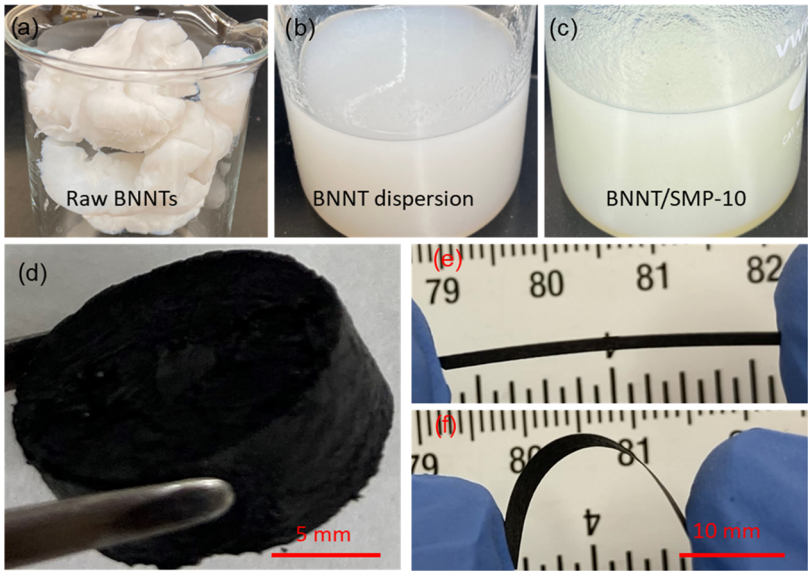

Figure 1. (a–c) Photos showing the first three steps of the manufacturing process toward SiC-BNNT ceramic composites. (d) Photo of a SiC-BNNT monolith (10 wt % BNNTs) from pyrolysis at 1200 °C. (e, f) Photos of a flexible SiC-BNNT thin film (40 wt % BNNTs, ∼100 μm thick) before and after being flexed down to a nearly 5 mm radius.

pyrolysis of a PDC monolith needs to proceed slowly with very slow heating and cooling rates (as low as 1 °C min^{-1} or less).[13−15] The thickness of the PDC can be reduced to avoid nonuniform volume shrinking and stress accumulation.[16] Because of these challenges and limited solutions, a large and thick sample can require multiple cycles of precursor infiltration and pyrolysis (PIP).[17,18] Improving the throughput of ceramic parts by the PDC process is of great interest.

In this work, we demonstrated a strategy of incorporating percolated boron nitride nanotube (BNNT) networks to reinforce a polymer-derived silicon carbide (SiC) ceramic. We found that SiC-BNNT composites with a BNNT weight concentration of 10% or more survived pyrolysis with a 100% fabrication yield. In contrast, all control samples (without or with a low concentration of BNNT) catastrophically failed during pyrolysis. We also found that the addition of BNNT permitted much faster heating and cooling rates during pyrolysis (≥15 °C min^{-1}). Notably, high-quality thin-film and bulk SiC-BNNT composite samples have been fabricated from a single cycle of the pyrolysis process with no need for subsequent lengthy PIP cycles. The SiC-BNNT composite has demonstrated a greatly improved elastic modulus, fracture strength, ductility, and thermal shock resistance. No mechanical property degradation was observed after 100 thermal shock cycles using a 1100 °C propane torch for heating and an ice−water bath for fast cooling. By increasing the BNNT weight concentration to 40%, we obtained highly flexible SiC-BNNT thin films that can be bent to a small radius without failure.

DISCUSSION

To prepare the SiC-BNNT composites, BNNTs[19] (Figure 1a) were dispersed in acetone with probe sonication. Scanning electron microscopy (SEM) and transmission electron microscopy (TEM) images of the BNNTs were shown in an earlier publication.[20] The BNNT/acetone dispersion (Figure 1b) was added with a commercial poly(carbosilane) preceramic polymer (SMP-10, Starfire) and thoroughly mixed with probe sonication. The SMP-10 polymer has about 15% weight loss after 1200−1800 °C pyrolysis. This weight loss is considered in this mixing step so that the final SiC-BNNT has the desired BNNT weight concentration. The BNNT/SMP-10 mixture (Figure 1c) was then dried out in an aluminum weighing pan to obtain BNNT/SMP-10 films of 20−500 μm thickness. The films were loaded into a stainless-steel mold and pressed at room temperature to obtain thicker BNNT/SMP-10 samples. The freshly prepared BNNT/SMP-10 samples were cured at 200 °C in the air for 12 h to obtain a green body that will then be transferred into a high-temperature graphite furnace for pyrolysis at 1200, 1500, or 1800 °C in a high-purity nitrogen atmosphere to convert the SMP-10 polymer into SiC and obtain the SiC-BNNT ceramic composite. In the pyrolysis, the temperature was increased from room temperature (∼25 °C) to 1200, 1500, or 1800 °C with a rate of 15 °C min^{-1}, maintained at that temperature for 1 h, and cooled down to ∼150 °C with a rate of 25 °C min^{-1}.

A thick SiC-BNNT sample is shown in Figure 1d that has 10 wt % BNNTs. Another thin-film disk with 10 wt % BNNTs was prepared and dropped onto the surface of an aluminum bar. Solid knocking sounds were heard (Supporting Video 1), suggesting that the SiC-BNNT sample in this work is dense without a significant volume of voids after pyrolysis. Figure 1e,f illustrates a thin-film sample, approximately 100 μm thick, containing 40 wt % BNNTs, which exhibits the capability to be bent significantly to a small radius. A video file can be found in the Supporting Information (Supporting Video 2) showing the flexing of the sample down to about a 5 mm radius for 6 cycles without breaking.

BNNT-reinforced PDCs have been previously reported by Jia et al.[21] In their work, the BNNTs were mixed with a cured silicon carbonitride (SiCN) preceramic polymer using a ball milling process, followed by mechanical pressing to shape the premixed powders into a circular disk and pyrolysis at 1000 °C (the curing, pressing and pyrolysis method). With 10 wt % BNNTs, they obtained PDC composites with a density of about 1.25 g cm^{-3} and a porosity of about 40%. In our approach, the preceramic polymer was shaped using film casting or molding before its curing, i.e., in a liquid or gel stage,

https://doi.org/10.1021/acsaenm.3c00524
ACS Appl. Eng. Mater. 2023, 1, 3205−3213

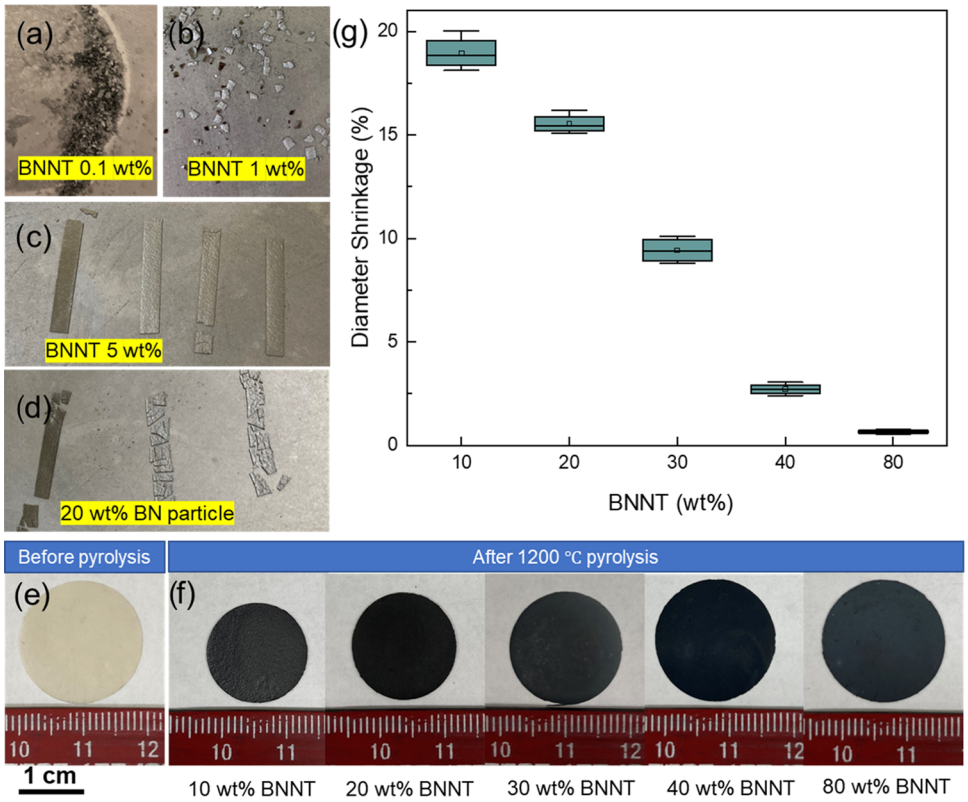

Figure 2. Photos of unsuccessful pyrolysis at 1200 °C for SiC-BNNT composites with (a) 0.1 wt % BNNTs, (b) 1 wt % BNNTs, and (c) 5 wt % BNNTs. (d) Photo of SiC-BN particle (20 wt % BN) composites after pyrolysis at 1200 °C. (e) Photo of one freshly prepared BNNT/SMP-10 sample with a diameter of about 0.75 in. (f) Photos of SiC-BNNT samples after 1200 °C pyrolysis. From left to right, the samples have BNNT weight concentrations of 10, 20, 30, 40, and 80%, respectively. (g) Plot shows the diameter shrinking of SiC-BNNT after 1200 °C pyrolysis compared with the starting BNNT/SMP-10 vs different BNNT weight concentrations. Four samples were measured in each BNNT weight ratio group.

to ensure a better connection of the preceramic polymer than the solid-state pressing. Therefore, our method (the casting, curing, and pyrolysis or molding, curing, and pyrolysis method) has achieved a much higher density of 2.30 g cm^{-3} after 1200 °C pyrolysis in the SiC-BNNT sample with 10 wt % BNNTs. A pore-free SiC sample from SMP-10 pyrolysis was calculated and experimentally measured to have a density of ~2.45 g cm^{-3} after 1200 °C pyrolysis,[22] and a three-dimensional hexagonal boron nitride (BN) has a density of about 2.1 g cm^{-3}. With both density values, we estimated that a fully dense SiC-BNNT composite with 10 wt % BNNTs should have a theoretical density of 2.41 g cm^{-3}, suggesting our SiC-BNNT composite has about 4.5% porosity. Given the fact that our BNNTs have a tubular architecture and a density slightly less than that of the three-dimensional hexagonal BN, the 2.41 g cm^{-3} theoretical density is likely overestimated. In this regard, our composite should have an even lower porosity than 4.5%, which is a lot less than the literature result by Jia et al.[21] The density of the SiC-BNNT (10 wt %) sample increased to 2.35 g cm^{-3} after 1500 °C pyrolysis but decreased to 2.06 g cm^{-3} after 1800 °C pyrolysis. In addition to the low porosity, our new manufacturing process allows us to fabricate thin-film ceramic composites with both rigid and flexible form factors.

The BNNT concentration is critical to preventing the PDC composite from cracking or shattering during pyrolysis. In our first attempt, we tested the pristine PDC with the SMP-10 preceramic polymer without BNNT incorporation. The SMP-10 liquid was cast onto a silicon wafer and baked at 200 °C in the air to cure the polymer (~20 μm). As shown in Figure S1, both samples that were made in the same batch severely cracked after the curing. With 0.1 wt % BNNT addition, all samples survived the curing step without cracking; however, they shattered into nearly powders after 1200 °C pyrolysis (Figure 2a). Increasing the BNNTs to 1 wt % still did not resolve this problem, although the samples shattered into slightly larger pieces after pyrolysis (Figure 2b). This situation was greatly improved when the BNNT concentration reached 5 wt %, by which half of the samples cracked, and the other half survived without cracking for all 4 samples we fabricated in a single batch (Figure 2c).

In comparison, three control samples with 20 wt % boron nitride (BN) particles in the SiC matrix cracked much more severely after pyrolysis than our 5 wt % BNNT samples (Figure 2d). While nanoparticle fillers to various PDC preceramic precursors have been well explored in the literature,[23] our observation here indicates that the use of high-aspect-ratio nanotubes has the advantages of a lower threshold percolation concentration and possibly a more effective load transfer between the PDCs and the fillers to mitigate crack formation during PDC pyrolysis.

We continued to prepare BNNT-preceramic polymer samples with different BNNT weight concentrations. Figure 2e shows a representative picture of freshly prepared BNNT/SMP-10 samples that were punched into a circular disk shape with a diameter of about 0.75 in. All samples with 10, 20, 30,

https://doi.org/10.1021/acsaenm.3c00524
ACS Appl. Eng. Mater. 2023, 1, 3205−3213

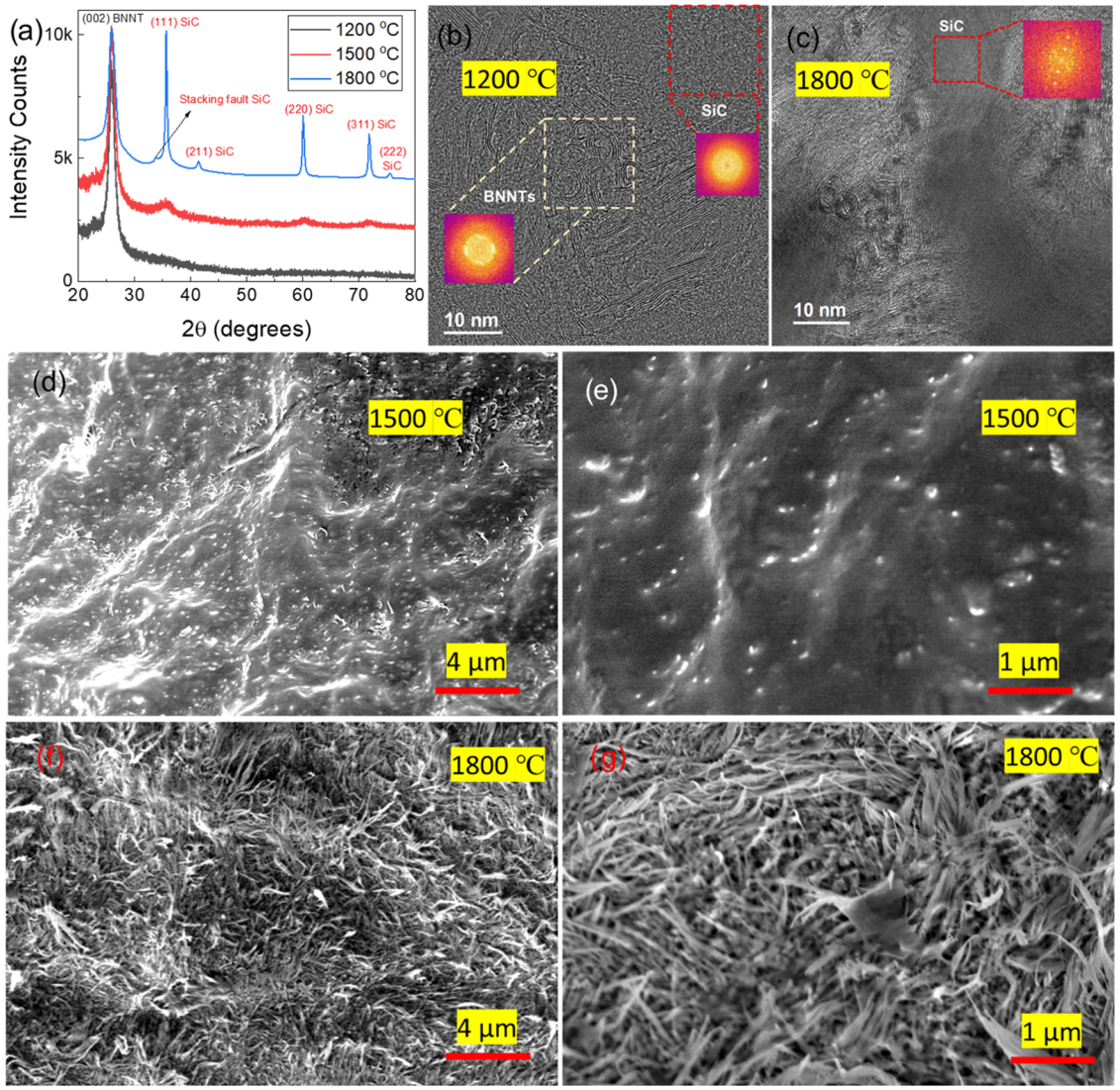

Figure 3. (a) XRD patterns of SiC-BNNT (20 wt %) composites after pyrolysis at 1200, 1500, and 1800 °C. (b, c) TEM images of SiC-BNNT (20 wt %) composites from 1200 and 1800 °C pyrolysis, respectively. The insets show the fast Fourier transform (FFT) of selected regions. (d, e) SEM images of SiC-BNNT (20 wt %) composites from 1500 °C pyrolysis. (f, g) SEM images of SiC-BNNT (20 wt %) composites from 1800 °C pyrolysis.

40, and 80 wt % BNNTs survived the pyrolysis process at 1200 °C with 100% yield. The pictures of those samples after pyrolysis are shown in Figure 2f. The plot in Figure 2g shows the relative diameter shrinkage after pyrolysis compared to the starting BNNT/SMP-10 for all samples with different BNNT concentrations. The average shrinkage is about 18.7% among four measured samples with 10 wt % BNNTs with a tendency of fast decrease with increasing BNNT concentration up to 40 wt %, after which the decreasing trend becomes much more gradual.

Figure 3a shows the X-ray diffraction (XRD) patterns of SiC-BNNT (20 wt %) samples after pyrolysis at 1200, 1500, and 1800 °C, respectively. All samples exhibit a strong diffraction peak at about 25.9° that can be attributed to the (002) basal plane of hexagonal BN or BNNTs.[24] This observation indicates that BNNTs were preserved even after 1800 °C pyrolysis. There are no noticeable diffraction peaks associated with SiC crystals after 1200 °C pyrolysis, indicating that the pyrolysis of the preceramic polymer at 1200 °C has mostly resulted in amorphous SiC. This statement is well supported by the TEM image in Figure 3b. Broad peaks start to appear in the 1500 °C pyrolysis sample at peak positions of 35.5, 60.1, and 71.8° that can be attributed to the (111), (220), and (311) planes of β-phase SiC, respectively.[25] With a further increase of the pyrolysis temperature to 1800 °C, the above diffraction peaks for the β-phase SiC become more intensified and narrower. Three new peaks have appeared at 33.7, 41.4, and 75.5° that are correlated with the stacking fault and (211) and (222) planes of β-phase SiC, respectively.[25] The improvement in crystallinity with 1800 °C pyrolysis is also supported by the TEM image in Figure 3c. The stacking fault in the SiC crystals can be seen in the TEM image in Figure S2.

The cross-sectional SEM images of the 1500 °C pyrolysis sample are shown in Figure 3d,e. BNNTs were seen to be tightly embedded in the SiC matrix. No microscopic pores are presented, which is in good agreement with our previously measured high density and calculated low porosity. On the contrary, the BNNTs appeared to largely separate from the SiC in the 1800 °C pyrolysis sample, as shown in Figure 3f,g, likely due to the crystallization of the SiC matrix that formed

https://doi.org/10.1021/acsaenm.3c00524
ACS Appl. Eng. Mater. 2023, 1, 3205−3213

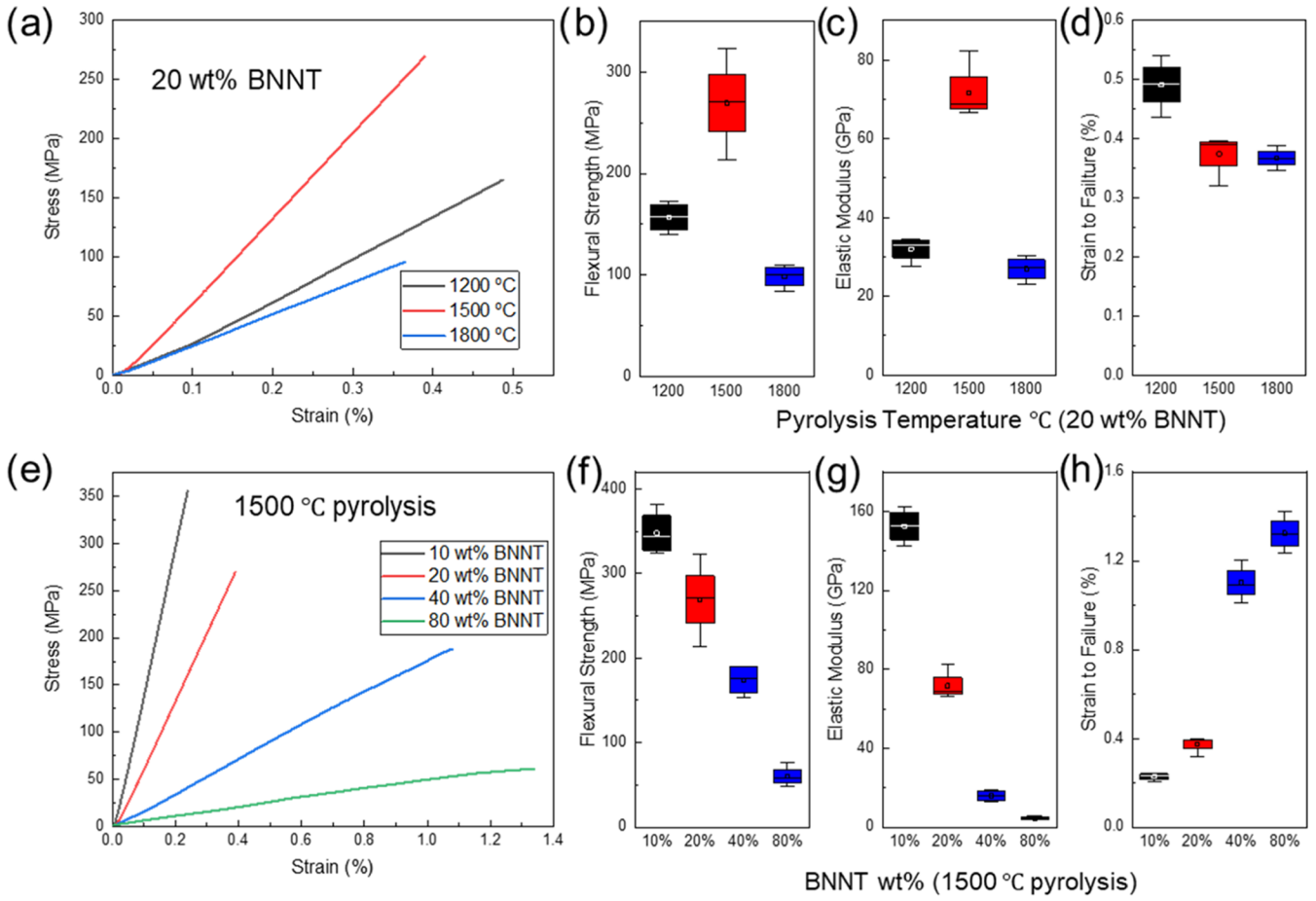

Figure 4. (a) Representative stress−strain characteristics from 3-point bending tests for SiC-BNNT (20 wt % BNNTs) samples with different pyrolysis temperatures. (b) Flexural strength, (c) elastic modulus, and (d) strain to failure of SiC-BNNT (20 wt % BNNTs) samples with different pyrolysis temperatures. Four samples were measured in each temperature group. (e) Representative stress−strain characteristics from 3-point bending tests for SiC-BNNT samples with different BNNT weight ratios after pyrolysis of at 1500 °C. (f) Flexural strength, (g) elastic modulus, and (h) strain to failure of SiC-BNNT samples (1500 °C pyrolysis) with different BNNT weight ratios. Four samples were measured in each BNNT weight ratio group.

submicron size particles surrounding the BNNTs (Figure 3g) and left many microscopic voids in the composites. It is argued that the thermal degradation of BNNTs at 1800 °C can negligibly contribute to void formation. As reported by Tank et al.,[20] the tubular structure of BNNTs remained wholly stable up to 1800 °C that is further confirmed by the XRD (Figure 3a) and TEM (Figure 3c) observations in this study. Overall, the void formation is attributed to the density decrease after 1800 °C pyrolysis, as discussed earlier.

The mechanical properties of the SiC-BNNT composites were evaluated with 3-point bending tests. We first tested SiC-BNNT samples with 20 wt % BNNTs and different pyrolysis temperatures. The results are presented in Figure 4a−d. In the four measured samples in each group, the 1200 °C pyrolysis samples have an average elastic modulus of 32 GPa, a maximum flexural strength of about 156 MPa, and a strain to failure value of about 0.49%. The elastic modulus and maximum flexural strength have improved to 72 GPa and 269 MPa, respectively, and the strain to failure reduced to about 0.37% after 1500 °C pyrolysis. The mechanical property changes are consistent with an increase of crystallinity for the SiC matrix from 1200 to 1500 °C pyrolysis temperature meant to make the composite stronger and stiffer. On the other hand, the 1800 °C pyrolysis samples exhibited the least elastic modulus of about 26.9 GPa and flexural strength of about 98 MPa. Such results are in support of the microscopic void formation, as shown in Figure 3f,g. The strain to failure remained at about 0.36% for the 1800 °C pyrolysis samples.

Using the 1500 °C pyrolysis temperature, we also prepared additional samples with BNNT weight concentrations of 10, 40, and 80%. Their 3-point bending test results, together with the 20% samples, are shown in Figure 4e−h. It is obvious that both the flexural strength and elastic modulus of the samples keep decreasing with increasing BNNT weight concentrations. Specifically, the average flexural strength is 347 MPa for the 10 wt % samples, decreasing to 269, 174, and 60 MPa in the 20, 40, and 80 wt % samples, respectively; the average elastic modulus is 152 GPa for the 10 wt % samples, decreasing to 72, 16, and 5 GPa in the 20, 40, and 80 wt % samples, respectively. It is worth noting that the 80 wt % sample suffers from high void contents as shown in the SEM images in Figure S3. This problem can partially contribute to the greatly reduced flexural strength and elastic modulus in the 80 wt % samples. It is also observed that the strain to failure keeps increasing with increasing BNNT weight concentrations. Specifically, the average strain to failure is 0.23% for the 10 wt % samples, increasing to 0.37, 1.1, and 1.3% in the 20, 40, and 80 wt % samples, respectively. The high strain-to-failure values obtained

https://doi.org/10.1021/acsaenm.3c00524
ACS Appl. Eng. Mater. 2023, 1, 3205−3213

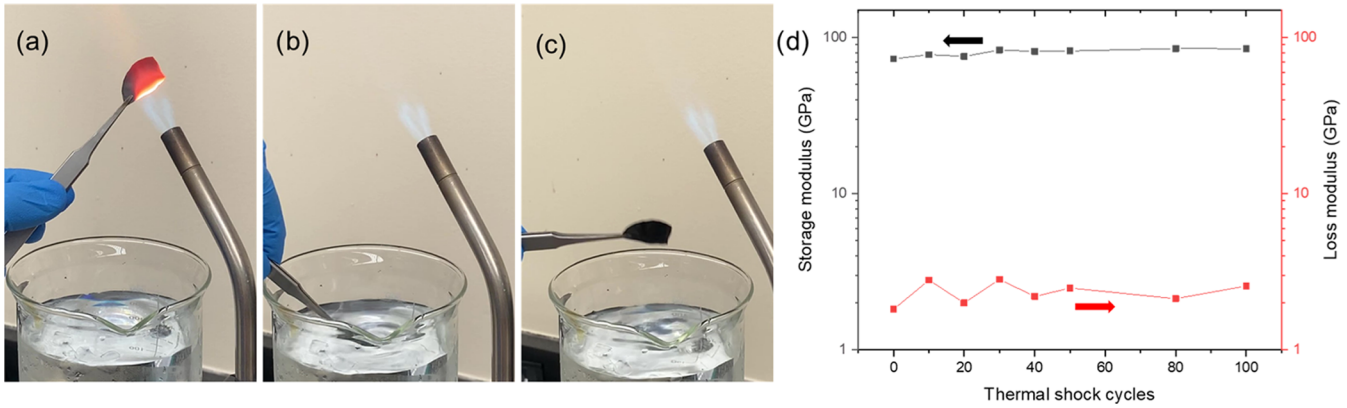

Figure 5. Photos showing the experimental setup and different measurement stages for evaluating the thermal shock resistance of one SiC-BNNT (20 wt % BNNTs, 1500 °C pyrolysis) composite sample. (a) Burning the sample with a propane torch in the air (~1100 °C), (b) within about half a second, moving the sample away from the flame and immersing it into an ice−water bath (~5 °C), (c) taking the survived sample out of the ice−water after one cycle of thermal sock testing. (d) Storage modulus and loss modulus vs numbers of thermal shock testing cycles for the sample in (a−c).

in the 40 and 80 wt % compositions lead to highly flexible thin-film ceramics, as shown in Figure 1g−i.

PDC bulk ceramics were reported with a relatively low elastic modulus and fracture strength due to their high porosity after pyrolysis. For instance, the best SiCN PDCs processed through the curing, pressing, and pyrolysis method had an elastic modulus from 105 to 118 GPa and fracture strength from 104 to 170 MPa.[26] Therefore, we have achieved a 30−50% improvement in modulus and a 2−3 times improvement in strength in our 1500 °C pyrolysis SiC-BNNT (10 wt %), which can be attributed to the low porosity in such samples.[27] It is worth noting that SiC (with 10 wt % Al_2O_3−Y_2O_3 additive) via liquid phase sintering at 2000 °C in an argon atmosphere was reported to exhibit an elastic modulus of ~430 GPa, fracture strength ~600 MPa, and strain to failure ~0.14%.[28] Both the modulus and fracture strength are significantly higher than those of PDCs, likely due to their much higher processing temperature than the best pyrolysis temperature (1500 °C) in our study. To support this argument, we noticed that de Mello et al. reported an elastic modulus of 209−228 GPa with a similar material composition of SiC (Al_2O_3−Y_2O_3) when 1750 °C was used for sintering.[29] Nonetheless, PDCs and their composites can be advantageous in manufacturing more versatile and customized product forms and geometries, accompanied by continuing efforts, including this work, to further reduce the mechanical property gap.[30]

Ceramics and their composites are often used in high-temperature environments, where rapid heating and cooling can be expected. We evaluated the thermal shock resistance of the SiC-BNNT composite with 20 wt % BNNTs and from 1500 °C pyrolysis. The sample was first burned with a propane torch in the air (Figure 5a) for 30 s. One K-type thermocouple was placed right next to the sample. The highest temperature reading from the thermocouple reached about 1100 °C after the 30 s burning. Within about half a second, the sample was moved away from the flame and quickly immersed in an ice−water bath (~5 °C) (Figure 5b). This quenching process corresponds to a temperature change rate of about 2190 °C s^{-1}. Surprisingly, the sample still survived after this quenching test (Figure 5c). A real-time video can be found in the Supporting Information (Supporting Video 3) to see the above-described heating−quenching cycles.

We also collected the storage modulus and the loss modulus of one sample after finishing a certain number of test cycles, and the data are plotted in Figure 5d. The storage modulus gradually increased from the initial about 73 GPa to about 84 GPa after the 30th heating−quenching cycle and then remained steady until the completion of 100 test cycles. The initial storage modulus improvement is possibly caused by a thermal annealing effect of SiC in the air that formed a conformal oxide overcoating and densified the surface of the test sample.[31] The loss modulus fluctuated slightly at around 2.2 GPa, leading to a loss tangent of 0.025 to 0.03 for all of the test cycles. It is worth noting that boron nitride has limited oxidation stability in the air (<1000 °C).[32] However, burning the SiC-BNNT PDCs with a propane torch in the above heating−quenching tests did not alter their appearance or mechanical properties. It is speculated that the BNNTs in the composite are well encapsulated and protected by the SiC matrix that has better temperature stability in the air.[31]

SiC is believed to have good thermal shock resistance due to its high thermal conductivity, low thermal expansion, and high strength. In one report, de Mello et al. studied the thermal shock resistance behaviors of a liquid phase sintered SiC (Al_2O_3−Y_2O_3) processed at 1950 °C. It was discovered that the elastic modulus had dropped by 15−25% after 20 thermal cycles with ΔT = ~725 °C.[29] In another study by Besisa et al. with SiC (Al_2O_3−Y_2O_3) sintered at 2080 °C, the fracture strength decreased by about 16.5% after 20 thermal cycles with ΔT = ~700 °C.[33] Comparing the above two studies with similar materials and temperature range of the thermal shock test, it is plausible to conclude that both elastic modulus and fracture strength can be used with good agreement to each other for quantifying thermal shock degradation.

The thermal shock resistance of SiC PDCs, however, has not been well studied in the literature. In one related report by Bergero et al., a silicon oxycarbide (SiCO) PDC composite reinforced with $MoSi_2$ microparticles was found to exhibit much worse thermal shock resistance than the above liquid phase sintered ceramics: for the SiCO−$MoSi_2$ samples, the fracture strength had reduced by about 75% after one thermal cycle with ΔT = 700 °C.[34] In contrast, our SiC-BNNT composite does not show any mechanical degradation (Figure 5d) even after 100 thermal cycles with ΔT = ~1100 °C. This greatly improved thermal shock resistance, as compared to

https://doi.org/10.1021/acsaenm.3c00524
ACS Appl. Eng. Mater. 2023, 1, 3205−3213

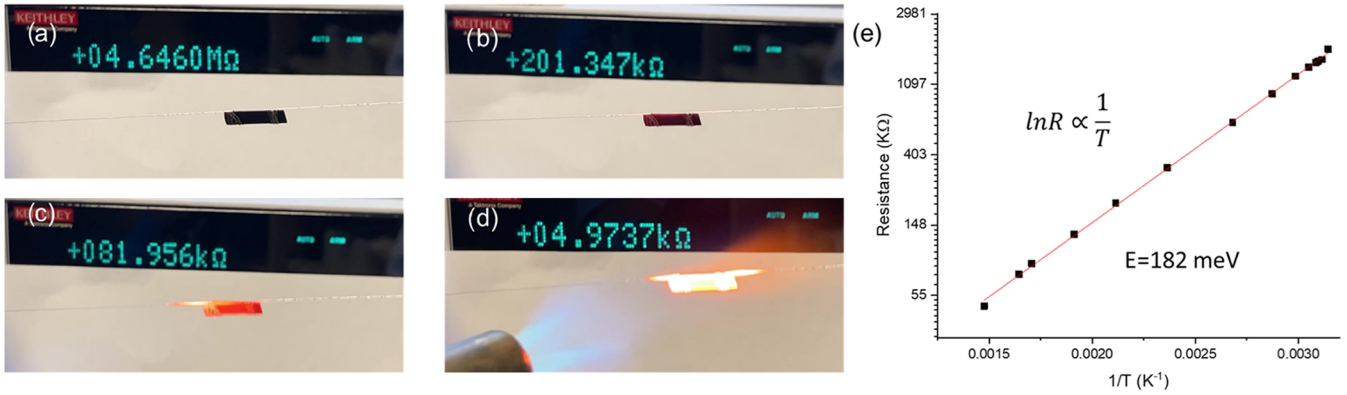

Figure 6. (a–d) Photos showing the experimental setup and resistance reading of one SiC-BNNT (20 wt %, 1500 °C pyrolysis) sample in the air while a propane torch was getting closer, and the sample became hotter and brighter. The sample had two platinum wound wires on both ends. The resistance was measured by a digital multimeter (Keithley 2400). (e) Logarithm of resistance (ln R) vs the reciprocal of absolute temperature ($1/T$) for one SiC-BNNT (20 wt %, 1500 °C pyrolysis) sample measured in a tube furnace in the air.

both PDCs and liquid phase sintered ceramics, can likely be attributed to the embedded BNNT network in the SiC matrix that effectively attenuates the propagation of microcracks during thermal shock testing.

The BNNT-reinforced SiC PDC composite can also be used to sense temperature through resistance changes. As shown in Figure 6 a–d, burning a sample (SiC-BNNT, 20 wt %, 1500 °C pyrolysis) with the propane torch in the air could reduce its resistance by nearly 1000 times. This resistance reduction can also be seen in one of the videos in the Supporting Information (Supporting Video 4). The same video also shows that moving the torch away then gradually restored its resistance back to the original value, accompanied by cooling of the sample. A quantitative plot in Figure 6e shows that the logarithm of resistance is proportional to the reciprocal of absolute temperature with an activation energy of 182 meV. This observation suggests that the conductivity in the SiC-BNNT PDC composite is limited by charge carrier concentration that exponentially increases with increasing temperatures. Given the high thermal shock resistance, the SiC-BNNT composites in this work can be useful for temperature sensing in addition to load-bearing structures in extreme environments with large and rapid changes in temperatures.

In conclusion, we demonstrated a strategy to use percolated BNNTs to accelerate the manufacturing of SiC PDC thin films and bulk monoliths. The BNNT network is essential for reinforcing the SiC matrix to sustain the large volume change during pyrolysis without cracking. The resulting SiC-BNNT composites showed low porosity and significantly improved mechanical properties. They also exhibit high thermal shock resistance. No mechanical degradation has been observed after 100 thermal shock cycles with a sudden temperature change of about 1100 °C. This extraordinary thermal shock resistance has greatly surpassed the state-of-the-art performance in ceramics of similar compositions fabricated from either liquid phase sintering or preceramic polymer pyrolysis. With the high thermal stability of the BNNTs, this approach can be more generic for future manufacturing of various high-temperature ceramics for extreme environment applications.

EXPERIMENTAL SECTION

BNNTs (SP10-R) were provided by BNNT, LLC. SMP-10 was purchased from Starfire Systems, Inc. Acetone (ACS reagent, ≥99.5%) and BN powder (~1 μm, 98%) were purchased from Sigma-Aldrich. All materials were used as received. The BNNT puffballs were dispersed in acetone by using a probe sonicator (Qsonica Q500 Sonicator) at 5 mg mL^{-1}. Pyrolysis was conducted in a high-temperature graphite furnace (Thermal Technologies HP-4560–20). The furnace was pumped to 10^{-5} Torr and then filled with high-purity nitrogen gas to atmospheric pressure. After that, a nitrogen gas flow of 2 SCFH was used throughout the pyrolysis process. SEM imaging was conducted using a Helios G4 UC (Thermo Fisher Scientific) with a 5 kV accelerating voltage. TEM images were collected using a JEM-ARM200cF (Cs corrected scanning/transmission electron microscope from JEOL) at 80 kV. A copper grid was used to support the TEM sample, which was prepared by a focused ion beam. A commercial X-ray diffractometer (SmartLab SE, Rigaku) with a Cu Kα radiation source was used for XRD analysis. The density of the composite was determined by using the Archimedes method. The porosity was calculated from the measured density value and the theoretical density value using $\left(1 - \frac{\rho_{measured}}{\rho_{theoretical}}\right)$. Mechanical stress–strain curves were obtained using a 3-point bending module with the DMA Q800 (TA Instruments, Inc.). The samples were 10 mm long, 5 mm wide, and 100 μm thick. Measurements were done with a controlled static force with a ramping rate of 0.1 N min^{-1}. Storage and loss moduli before and after thermal shock experiments were obtained using the same 3-point bending setup with a constant frequency of 1 Hz.

ASSOCIATED CONTENT

Supporting Information

The Supporting Information is available free of charge at https://pubs.acs.org/doi/10.1021/acsaenm.3c00524.

Photos of SMP-10 films without BNNTs on silicon wafer (Figure S1); TEM image of SiC-BNNT with 1800 °C pyrolysis (Figure S2); and SEM images of SiC-BNNT with 80 wt % BNNTs (Figure S3) (PDF)

Sample dropping onto aluminum bar (AVI)

Flexing of the sample (AVI)

Heating–quenching cycles (AVI)

Temperature sensing (AVI)

AUTHOR INFORMATION

Corresponding Author

Zhibin Yu − *Department of Industrial and Manufacturing Engineering, FAMU-FSU College of Engineering and High-Performance Materials Institute, Florida State University,*

https://doi.org/10.1021/acsaenm.3c00524
ACS Appl. Eng. Mater. 2023, 1, 3205–3213

Tallahassee, Florida 32310, United States; orcid.org/0000-0002-4630-4363; Email: zyu@eng.famu.fsu.edu

Authors

Haoran Li − *Department of Industrial and Manufacturing Engineering, FAMU-FSU College of Engineering and High-Performance Materials Institute, Florida State University, Tallahassee, Florida 32310, United States*

Leila Shahriari − *Department of Industrial and Manufacturing Engineering, FAMU-FSU College of Engineering and High-Performance Materials Institute, Florida State University, Tallahassee, Florida 32310, United States*

Yash Khandwani − *Department of Industrial and Manufacturing Engineering, FAMU-FSU College of Engineering and High-Performance Materials Institute, Florida State University, Tallahassee, Florida 32310, United States*

Samuel Talevich − *High-Performance Materials Institute, Florida State University, Tallahassee, Florida 32310, United States*

Aspen Reyes − *Department of Industrial and Manufacturing Engineering, FAMU-FSU College of Engineering and High-Performance Materials Institute, Florida State University, Tallahassee, Florida 32310, United States*

Rebekah Sweat − *Department of Industrial and Manufacturing Engineering, FAMU-FSU College of Engineering and High-Performance Materials Institute, Florida State University, Tallahassee, Florida 32310, United States*

Keyou Mao − *Department of Industrial and Manufacturing Engineering, FAMU-FSU College of Engineering, Florida State University, Tallahassee, Florida 32310, United States; National High Magnetic Field Laboratory, Tallahassee, Florida 32310, United States*

Lyndsey R. Scammell − *BNNT Materials LLC, Newport News, Virginia 23606, United States;* orcid.org/0000-0002-7133-7546

R. Roy Whitney − *BNNT Materials LLC, Newport News, Virginia 23606, United States*

Jin Gyu Park − *Department of Industrial and Manufacturing Engineering, FAMU-FSU College of Engineering and High-Performance Materials Institute, Florida State University, Tallahassee, Florida 32310, United States*

Qiang Wu − *Department of Industrial and Manufacturing Engineering, FAMU-FSU College of Engineering and High-Performance Materials Institute, Florida State University, Tallahassee, Florida 32310, United States*

Zhiyong Liang − *Department of Industrial and Manufacturing Engineering, FAMU-FSU College of Engineering and High-Performance Materials Institute, Florida State University, Tallahassee, Florida 32310, United States;* orcid.org/0000-0001-5099-9957

Complete contact information is available at: https://pubs.acs.org/10.1021/acsaenm.3c00524

Notes

The authors declare no competing financial interest.

■ ACKNOWLEDGMENTS

Z.Y. thanks the NNSA Minority Serving Institution Partnership Program (MSIPP) (award #DE-NA0004004) for partial summer support. TEM work was performed at the National High Magnetic Field Laboratory, which is supported by National Science Foundation Cooperative Agreement No. DMR-1644779 and the State of Florida.

■ REFERENCES

(1) Prameela, S. E.; Pollock, T. M.; Raabe, D.; Meyers, M. A.; Aitkaliyeva, A.; Chintersingh, K. L.; Cordero, Z. C.; Graham-Brady, L. Materials for extreme environments. *Nat. Rev. Mater.* **2023**, *8* (2), 81−88.

(2) Padture, N. P. Advanced structural ceramics in aerospace propulsion. *Nat. Mater.* **2016**, *15* (8), 804−809.

(3) Zheng, J. M.; Reed, J. S. Effects of Particle Packing Characteristics on Solid-State Sintering. *J. Am. Ceram. Soc.* **1989**, *72* (5), 810−817.

(4) German, R. M.; Suri, P.; Park, S. Review: liquid phase sintering. *J. Mater. Sci.* **2009**, *44* (1), 1−39.

(5) Weston, J. E.; Pratt, P. L. Crystallization of Grain-Boundary Phases in Hot-Pressed Silicon-Nitride Materials. 2. Mechanical-Properties of Materials. *J. Mater. Sci.* **1978**, *13* (10), 2147−2156.

(6) Colombo, P.; Mera, G.; Riedel, R.; Soraru, G. D. Polymer-Derived Ceramics: 40 Years of Research and Innovation in Advanced Ceramics. *J. Am. Ceram. Soc.* **2010**, *93* (7), 1805−1837.

(7) Eckel, Z. C.; Zhou, C. Y.; Martin, J. H.; Jacobsen, A. J.; Carter, W. B.; Schaedler, T. A. 3D PRINTING Additive manufacturing of polymer-derived ceramics. *Science* **2016**, *351* (6268), 58−62.

(8) Yajima, S.; Hayashi, J.; Omori, M.; Okamura, K. Development of a Silicon-Carbide Fiber with High-Tensile Strength. *Nature* **1976**, *261* (5562), 683−685.

(9) Delcamp, J. H.; Martin, K. L.; Posey, N. D.; Acord, K. A.; Thompson, C. M.; Dickerson, M. B. Preceramic Polymers Grafted to SiO2 Nanoparticles via Metal Coordination Pyrolyzing with High Ceramic Yields: Implications for Aerospace Propulsion and Biomedical Coatings. *ACS Appl. Nano Mater.* **2023**, *6*, 3661−3674, DOI: 10.1021/acsanm.2c05394.

(10) Lodhe, M.; Babu, N.; Selvam, A.; Balasubramanian, M. Synthesis and characterization of high ceramic yield polycarbosilane precursor for SiC. *J. Adv. Ceram.* **2015**, *4* (4), 307−311.

(11) Wang, C. W.; Ping, W. W.; Bai, Q.; Cui, H. C.; Hensleigh, R.; Wang, R. L.; Brozena, A. H.; Xu, Z. P.; Dai, J. Q.; Pei, Y.; Zheng, C. L.; Pastel, G.; Gao, J. L.; Wang, X. Z.; Wang, H.; Zhao, J. C.; Yang, B.; Zheng, X. Y.; Luo, J.; Mo, Y. F.; Dunn, B.; Hu, L. B. A general method to synthesize and sinter bulk ceramics in seconds. *Science* **2020**, *368* (6490), 521−526.

(12) Okoroanyanwu, U.; Bhardwaj, A.; Einck, V.; Ribbe, A.; Hu, W. G.; Rodriguez, J. M.; Schmidt, W. R.; Watkins, J. J. Rapid Preparation and Electrochemical Energy Storage Applications of Silicon Carbide and Silicon Oxycarbide Ceramic/Carbon Nanocomposites Derived Via Flash Photothermal Pyrolysis of Organosilicon Preceramic Polymers. *Chem. Mater.* **2021**, *33* (2), 678−694.

(13) Ly, H. Q.; Taylor, R.; Day, R. J.; Heatley, F. Conversion of polycarbosilane (PCS) to SiC-based ceramic - Part II - Pyrolysis and characterisation. *J. Mater. Sci.* **2001**, *36* (16), 4045−4057.

(14) Nishimura, T.; Haug, R.; Bill, J.; Thurn, G.; Aldinger, F. Mechanical and thermal properties of Si-C-N material from polyvinylsilazane. *J. Mater. Sci.* **1998**, *33* (21), 5237−5241.

(15) Shen, C.; Barrios, E.; Zhai, L. Bulk Polymer-Derived Ceramic Composites of Graphene Oxide. *ACS Omega* **2018**, *3* (4), 4006−4016.

(16) Colombo, P.; Paulson, T. E.; Pantano, C. G. Synthesis of silicon carbide thin films with polycarbosilane (PCS). *J. Am. Ceram. Soc.* **2005**, *80* (9), 2333−2340.

(17) Moraes, K. V.; Interrante, L. V. Processing, fracture toughness, and vickers hardness of allylhyd ridopolycarbosilane-derived silicon carbide. *J. Am. Ceram. Soc.* **2003**, *86* (2), 342−346.

(18) Lee, S. H.; Weinmann, M.; Aldinger, F. Processing and properties of C/Si-B-C-N fiber-reinforced ceramic matrix composites

prepared by precursor impregnation and pyrolysis. *Acta Mater.* **2008**, *56* (7), 1529−1538.
(19) Smith, M. W.; Jordan, K. C.; Park, C.; Kim, J. W.; Lillehei, P. T.; Crooks, R.; Harrison, J. S. Very long single- and few-walled boron nitride nanotubes via the pressurized vapor/condenser method. *Nanotechnology* **2009**, *20* (50), No. 505604, DOI: 10.1088/0957-4484/20/50/505604.
(20) Tank, M. J.; Reyes, A. N.; Park, J. G.; Scammell, L. R.; Smith, M. W.; De Leon, A.; Sweat, R. D. Extreme thermal stability and dissociation mechanisms of purified boron nitride nanotubes: implications for high-temperature nanocomposites. *ACS Appl. Nano Mater.* **2022**, *5* (9), 12444−12453.
(21) Jia, Y. J.; Ajayi, T. D.; Xu, C. Y. Dielectric properties of polymer-derived ceramic reinforced with boron nitride nanotubes. *J. Am. Ceram. Soc.* **2020**, *103* (10), 5731−5742.
(22) Key, T. S.; Patel, D. K.; Wilks, G. B.; Cinibulk, M. K. Modeling the pyrolysis of preceramic polymers: A kinetic study of the polycarbosilane SMP-10. *J. Eur. Ceram Soc.* **2021**, *41* (13), 6356−6365.
(23) Mirkhalaf, M.; Sarvestani, H. Y.; Yang, Q.; Jakubinek, M. B.; Ashrafi, B. A comparative study of nano-fillers to improve toughness and modulus of polymer-derived ceramics. *Sci. Rep* **2021**, *11* (1), No. 6951.
(24) Amin, M. S.; Atwater, B.; Pike, R. D.; Williamson, K. E.; Kranbuehl, D. E.; Schniepp, H. C. High-Purity Boron Nitride Nanotubes via High-Yield Hydrocarbon Solvent Processing. *Chem. Mater.* **2019**, *31* (20), 8351−8357.
(25) Luo, G. Q.; Zhang, Z.; Hu, J. N.; Zhang, J.; Sun, Y.; Shen, Q.; Zhang, L. M. Study on Rheological Behavior of Micro/Nano-Silicon Carbide Particles in Ethanol by Selecting Efficient Dispersants. *Materials* **2020**, *13* (7), No. 1496, DOI: 10.3390/ma13071496.
(26) Sujith, R.; Jothi, S.; Zimmermann, A.; Aldinger, F.; Kumar, R. Mechanical behaviour of polymer derived ceramics - a review. *Int. Mater. Rev.* **2021**, *66* (6), 426−449.
(27) Shah, S. R.; Raj, R. Mechanical properties of a fully dense polymer derived ceramic made by a novel pressure casting process. *Acta Mater.* **2002**, *50* (16), 4093−4103.
(28) Zhang, G. J.; Ohji, T. Effect of BN content on elastic modulus and bending strength of SiC-BN in situ composites. *J. Mater. Res.* **2000**, *15* (9), 1876−1880.
(29) de Mello, R. M.; Bressiani, A. H. d. A. *Thermal Shock Resistance of Liquid Phase Sintered SiC*; Materials Science Forum, Trans Tech Publ, 2017; pp 103−108.
(30) Dyatkin, B.; Laskoski, M. Commercially scalable, single-step polymer-derived reaction bonding synthesis of refractory ceramics. *Am. Ceram. Soc. Bull.* **2020**, *99* (7), 30−35.
(31) Roy, J.; Chandra, S.; Das, S.; Maitra, S. Oxidation Behaviour of Silicon Carbide - a Review. *Rev. Adv. Mater. Sci.* **2014**, *38* (1), 29−39.
(32) Kostoglou, N.; Polychronopoulou, K.; Rebholz, C. Thermal and chemical stability of hexagonal boron nitride (h-BN) nano-platelets. *Vacuum* **2015**, *112*, 42−45.
(33) Besisa, D. H. A.; Ewais, E. M. M.; Ahmed, Y. M. Z.; Elhosiny, F. I.; Fend, T.; Kuznetsov, D. V. Thermal shock resistance of pressureless sintered SiC/AlN ceramic composites. *Mater. Res. Express* **2018**, *5* (1), No. 015506, DOI: 10.1088/2053-1591/aaa2c2.
(34) Bergero, L.; Sglavo, V. M.; Soraru, G. D. Processing and thermal shock resistance of a polymer-derived $MoSi_2$/SiCO ceramic composite. *J. Am. Ceram. Soc.* **2005**, *88* (11), 3222−3225.

https://doi.org/10.1021/acsaenm.3c00524
ACS Appl. Eng. Mater. 2023, 1, 3205−3213